Molecular Therapy
Oncolytics
Original Article

Dual-targeting vaccine of FGL1/CAIX exhibits potent anti-tumor activity by activating DC-mediated multi-functional CD8 T cell immunity

Dafei Chai,[1,2,3,7] Dong Qiu,[1,4,7] Xiaoqing Shi,[5] Jiage Ding,[1,2,3] Nan Jiang,[1,4] Zichun Zhang,[1,4] Jiawei Wang,[1,2,3] Jie Yang,[1,2,3] Pengli Xiao,[6] Gang Wang,[1,2,3] and Junnian Zheng[2,3]

[1]Cancer Institute, Xuzhou Medical University, Xuzhou, Jiangsu, China; [2]Jiangsu Center for the Collaboration and Innovation of Cancer Biotherapy, Cancer Institute, Xuzhou Medical University, Xuzhou, Jiangsu, China; [3]Center of Clinical Oncology, Affiliated Hospital of Xuzhou Medical University, Xuzhou, Jiangsu, China; [4]Department of Urology, Affiliated Hospital of Xuzhou Medical University, Xuzhou, Jiangsu, China; [5]Department of General Surgery, Affiliated Hospital of Xuzhou Medical University, Xuzhou, Jiangsu, China; [6]Department of Hematology, Luoyang Central Hospital Affiliated to Zhengzhou University, Luoyang, Henan, China

Tumor DNA vaccine as an effective therapeutic approach can induce systemic immunity against malignant tumors, but its therapeutic effect is still not satisfactory in advanced renal cancer. Herein, a novel DNA vaccine containing dual antigens of fibrinogen-like protein 1 (FGL1) and carbonic anhydrase IX (CAIX) was developed and intramuscularly delivered by PLGA/PEI nanoparticles for renal cancer therapy. Compared with PLGA/PEI-pCAIX immunization, PLGA/PEI-pFGL1/pCAIX co-immunization significantly inhibited the subcutaneous tumor growth and promoted the differentiation and maturation of $CD11c^+$ DCs and $CD11c^+CD11b^+$ DCs subset. Likewise, the increased capabilities of CD8 T cell proliferation, CTL responses, and multi-functional $CD8^+$ T cell immune responses were observed in PLGA/PEI-pFGL1/pCAIX vaccine group. Interestingly, depletion of $CD8^+$ T cells by using CD8 mAb resulted in a loss of anti-tumor function of PLGA/PEI-pFGL1/pCAIX vaccine, suggesting that the anti-tumor activity of the vaccine was dependent on $CD8^+$ T cell immune responses. Furthermore, PLGA/PEI-pFGL1/pCAIX co-immunization also suppressed the lung metastasis of tumor mice by enhancing the multi-functional $CD8^+$ T cell responses. Therefore, these results indicate that PLGA/PEI-pFGL1/pCAIX vaccine could provide an effective protective effect for renal cancer by enhanced DC-mediated multi-functional $CD8^+$ T cell immune responses. This vaccine strategy offers a potential approach for solid or metastatic tumor treatment.

INTRODUCTION

Renal cell cancer (RCC), referred to as renal cancer, is the most common malignant tumor in the urinary system, accounting for 60% to 80% of all primary kidney cancers.[1] In 2018, kidney cancer caused more than 175,000 deaths, and its incidence is increasing globally.[2] Radical renal cancer resection is an effective method for the treatment of early renal cancer. Unfortunately, 25% to 30% of renal cancer patients have already developed distant metastases at the time of diagnosis.[3] The treatment of advanced renal cancer is mainly based on anti-vascular factors, cytokines, monoclonal antibodies, and kinase inhibitors,[4,5] but there are problems such as high cost, large side effects, and high drug resistance that lead to short disease control processes.[6] Patients with advanced metastatic renal cancer show a high rate of metastasis and recurrence with no effective therapeutic approach.[7] Therefore, there is an urgent need to develop new drugs and approaches for the treatment of advanced renal cancer.

Tumor immunotherapy has developed rapidly in recent years, but the treatment of tumors is still one of the world's problems.[8,9] As an important component of tumor immunotherapy, therapeutic tumor vaccines have attracted much attention and have been used as an important breakthrough in the treatment of solid tumors.[10] Among them, gene vaccines play an important role in tumor vaccines, and have become one of the hot spots researched in recent years.[11] DNA-encoding cytokines, transcription factors, or antigens are fused into a plasmid DNA of genetic engineering vaccine, which effectively improves vaccine antigen immunogenicity and causes a strong immune response.[12,13] The key factors, including tumor antigen, vaccine delivery system, and adjuvant, are important for DNA vaccine to induce antigen-specific immunity for killing tumor antigen cells.

Carbonic anhydrase IX (CAIX), also known as G250, is one of the isomers of the carbonic anhydrase family. CAIX is a transmembrane glycoprotein composed of acidic amino acids, which catalyzes the conversion of carbon dioxide into bicarbonate.[14,15] CAIX antigen is expressed in about 90% of RCCs, and is also upregulated in breast cancer, oral squamous cell carcinoma, mesothelioma, head-and-neck cancer,

Received 30 July 2021; accepted 27 November 2021;
https://doi.org/10.1016/j.omto.2021.11.017.

[7]These authors contributed equally

Correspondence: Gang Wang, PhD, Cancer Institute, Xuzhou Medical University, 84 West Huaihai Road, Xuzhou, Jiangsu 221002, China.
E-mail: wangg@xzhmu.edu.cn
Correspondence: Junnian Zheng, Cancer Institute, Xuzhou Medical University, 84 West Huaihai Road, Xuzhou, Jiangsu 221002, China.
E-mail: jnzheng@xzhmu.edu.cn

etc.[16–20] In normal kidney tissues or other normal tissues, CAIX expression is almost not detected, but only a small amount of CAIX expression is detected in gastric mucosa, gut epithelial tissue, and gallbladder epithelial cells.[21,22] Overexpressing CAIX promotes the malignant behaviors of tumor by reducing the adhesion of cancer cells, increasing the migration and invasion of cancer cells, thus it is called renal cancer-associated antigen that is used as a target for renal cancer treatment.[23,24] Studies have reported that various vaccines based on CAIX antigen can effectively stimulate antigen-specific immune responses and inhibit the growth of renal cancer.[25,26] The preliminary results of our research group also confirm that CAIX vaccine with the help of the adjuvant can induce antigen-specific multi-functional CD8 T cell immune response and suppress the tumor growth of renal cancer.[27] These results indicate that the developed DNA vaccine based on CAIX antigen is an effective way to treat renal cancer.

Fibrinogen-like protein 1 (FGL1), also called hepatocyte-derived fibrinogen-like protein-1, is a member of the fibrinogen family.[28] Recently, overexpression of FGL1 has been reported in many solid tumors, and its expression is associated with a shorter 5-year overall survival rate.[29] The expression of FGL1 not only affects the regeneration of hepatocytes, but also regulates the growth and proliferation of tumor cells.[30,31] The research shows that FGL1 is the main inhibitory ligand of lymphocyte activation gene 3 (LAG-3), which can inhibit antigen-specific T cell responses through the interaction of FGL1/LAG-3.[32] Blockade of the inhibiting signal of FGL1/LAG-3 by knockout of FGL1 or function-blocking monoclonal antibody (mAb) can enhance T cell immunity in the tumor microenvironment and inhibit tumor growth.[32] Therefore, we infer that FGL1 as an adjuvant or antigen of DNA vaccine can enhance the specific T cell immune responses.

This study intends to construct a PLGA/PEI-pFGL1/pCAIX nanoparticle-based dual-targeting vaccine, and to verify its therapeutic effect in renal cancer treatment through *in vivo* and *in vitro* experiments. Furthermore, the mechanism of action of the PLGA/PEI-pFGL1/pCAIX nano-vaccine was also explored in renal cancer therapy. This study provides a new approach for the immunotherapy of renal cancer and will also lay the experimental foundation for its application in other malignant tumors.

RESULTS

The vaccine antigens of FGL1 or CAIX are efficiently expressed *in vitro* and *in vivo*

In order to test whether the vaccine antigens could be effectively expressed by PLGA/PEI-pFGL1/pCAIX vaccine *in vitro*, PLGA/PEI-pFGL1 or PLGA/PEI-pCAIX was transfected into HEK-293T cells, and flow cytometry technique was used to detect their transfection efficiency. Compared with PLGA/PEI-Vector group, PLGA/PEI-pFGL1 and PLGA/PEI-pCAIX group showed the significantly increased expression, and the percentages of FGL1 and CAIX expression were 86.9% and 91.2%, respectively (Figures 1A and 1B), the difference is statistically significant ($p < 0.0001$) (Figures 1C and 1D). In order to detect whether the PLGA/PEI-pFGL1 and PLGA/PEI-pCAIX nano-vaccine could effectively express the antigen protein *in vivo*, we vaccinated the quadriceps femoris muscle of mice, and then extracted the muscle cell protein for western blot analysis. The results showed that FGL1 and CAIX proteins could both be effectively expressed *in vivo* (Figures 1E and 1F), the difference is statistically significant ($p < 0.0001$) (Figures 1G and 1H). In summary, these results indicate that PLGA/PEI-pFGL1 and PLGA/PEI-pCAIX nanoparticles can efficiently express antigen proteins *in vitro* or *in vivo*.

PLGA/PEI-pFGL1/pCAIX nano-vaccine exhibits a potent anti-tumor activity in mouse subcutaneous tumor model

Renca cells were infected with hCAIX-expressing lentivirus for the establishment of hCAIX-Renca cell line. Compared with control cells, hCAIX-Renca cells showed a significant increase of CAIX expression detected by flow cytometry (Figures 2A and 2B). In order to evaluate the therapeutic effect of the PLGA/PEI-pFGL1/pCAIX nano-vaccine, the subcutaneous tumor models inoculated with hCAIX-Renca were immunized with various vaccines. Tumor volumes were monitored weekly, and tumor weights were detected on day 42 after tumor inoculation. Tumor growth was significantly inhibited in PLGA/PEI-pFGL1/pCAIX vaccine-immunized mice compared with PLGA/PEI-pCAIX vaccine-immunized mice (Figures 2C–2E). Similarly, the reduced tumor weight and increased tumor inhibition rate were observed in PLGA/PEI-pFGL1/pCAIX immunization group (Figures 2F and 2G). Furthermore, the toxic and side effects of the PLGA/PEI-pFGL1/pCAIX nano-vaccine were also evaluated by monitoring the serum levels of interleukin (IL)-6 in mice at day 2 and day 7 after vaccine inoculation. Compared with PLGA/PEI-Vector group, PLGA/PEI-pFGL1/pCAIX group showed the increased levels of IL-6 measured by ELISA in serum on day 2 after vaccination. However, the inflammatory cytokine IL-6 levels were back to basal concentrations on day 7 (Figure 2H), suggesting that a transient inflammatory reaction was induced by the vaccine. Next, H&E staining was performed on the heart, kidney, and liver of each group of mice. The results showed that there was no obvious immune response and inflammatory injury demonstrated by normal pathological tissue of heart, kidney, and liver in PLGA/PEI-pFGL1/pCAIX-immunized mice (Figure 2I) indicated its low toxicity. In summary, PLGA/PEI-pFGL1/pCAIX co-immunization effectively prevents the progression of renal cancer without obvious side effects.

PLGA/PEI-pFGL1/pCAIX nano-vaccine promotes the induction and maturation of DCs in tumor-bearing mice

Dendritic cells (DCs) are the body's most powerful full-time antigen-presenting cells, which can efficiently ingest, process, and present antigens.[33] Mature DCs can effectively activate the initial T cells, enabling the body to start, regulate, and maintain the status of the immunity response.[34] In order to investigate the effect of the PLGA/PEI-pFGL1/pCAIX nano-vaccine on the function of DCs *in vivo*, we collected the spleen cells from each vaccine-immunized mouse and performed relevant tests. The results of flow cytometry showed that the percentages of $CD11c^+$ DCs or $CD11b^+CD11c^+$ DCs were significantly increased in the PLGA/PEI-pFGL1/pCAIX co-immunization group compared with the PLGA/PEI-pCAIX single immunization

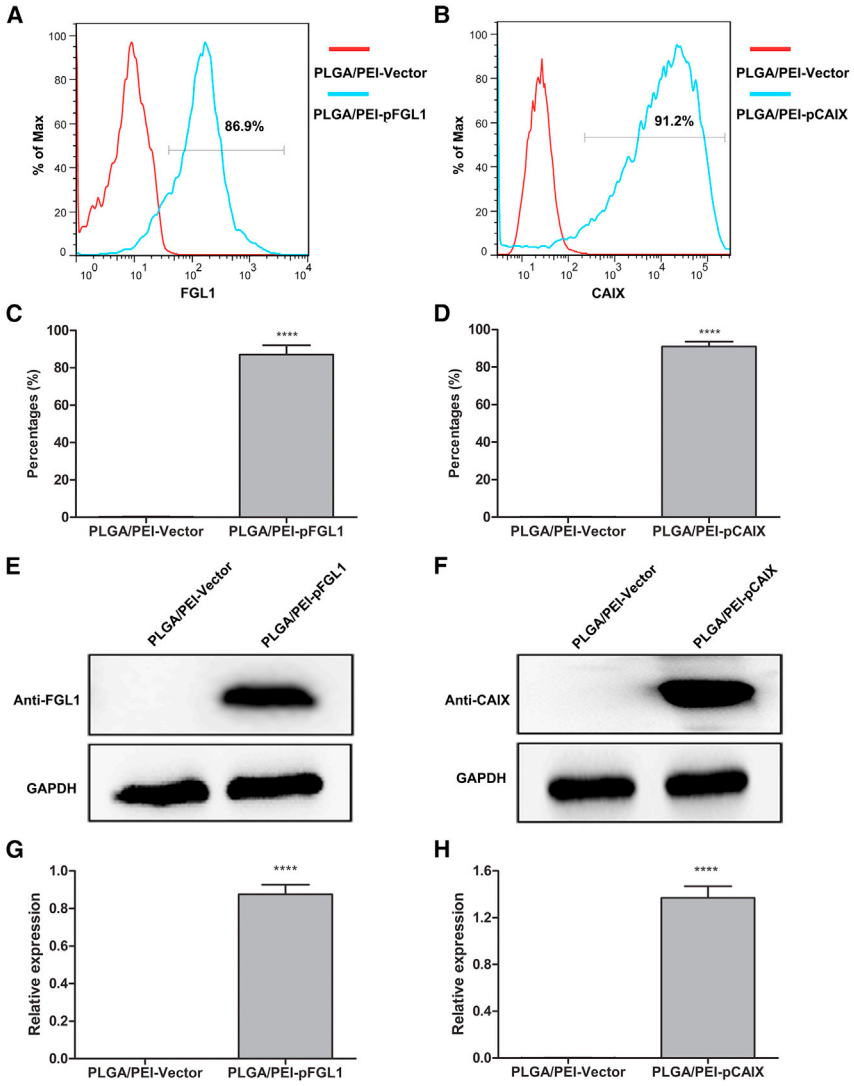

Figure 1. The expression of PLGA/PEI-pFGL1 and PLGA/PEI-pCAIX vaccine

293T cells were transfected with PLGA/PEI-pFGL1, PLGA/PEI-pCAIX, or PLGA/PEI-Vector for 48 h, and then cells were subjected to flow cytometry analysis using anti-FGL1, anti-CAIX, and control antibody, respectively. (A and B) The expression of FGL1 or CAIX in transfected 293T cells. One representative flow cytometry result was shown for per group. (C and D) Statistical analysis of the frequencies of FGL1 or CAIX expressing cells in (A and B). PLGA/PEI-pFGL1, PLGA/PEI-pCAIX, and PLGA/PEI-Vector nanoparticles were used to immunize BALB/c mice into muscles. (E and F) After 3 days, muscle cell proteins were extracted, and CAIX and FGL1 protein expression was detected by western blot, PLGA/PEI-Vector group as the control. (G and H) Quantification of FGL1 or CAIX expression by densitometry in (E and F). Data are from one representative experiment of three performed and presented as the mean ± SD. The different significance was set at ****$p < 0.0001$.

group (Figures 3A–3D). Of note, the activation changes of DCs were determined by flow cytometry; the results showed that the expression of CD80, CD86, or MHCII on DCs in the PLGA/PEI-pFGL1/pCAIX co-immunization group was higher than that in the PLGA/PEI-pCAIX immunization group (Figures 3E–3H). These results indicate that the PLGA/PEI-pFGL1/pCAIX nano-vaccine could promote the induction of DCs *in vivo* and increase their maturation.

PLGA/PEI-pFGL1/pCAIX nano-vaccine enhances antigen-specific CD8$^+$ T cell immune responses

Tumor vaccines can induce antigen-specific CD8 T cell responses to kill tumor cells, thus exerting the anti-tumor effect.[35] In order to evaluate whether PLGA/PEI-pFGL1/pCAIX nano-vaccine enhanced antigen-specific CD8$^+$ T cell immune responses, the proliferation of CD8$^+$ T cells, killing effect of cytotoxic T lymphocytes (CTL) and induction of functional interferon (IFN)-γ^+CD8$^+$ T cell were assessed in various immunization groups. As shown in Figures 4A and 4B, PLGA/PEI-pFGL1/pCAIX co-immunization group showed a higher CD8 T cell proliferation reaction than PLGA/PEI-pCAIX immunization group. The killing curve of PLGA/PEI-pFGL1/pCAIX vaccine group dropped faster than other vaccine group, and the tumor cells were basically killed in about 96 h (lower cell index), indicating that lymphocytes from mice immunized with PLGA/PEI-pFGL1/pCAIX vaccine showed a higher killing capacity against hCAIX-Renca cells than those from mice immunized with PLGA/PEI-pCAIX vaccine (Figures 4C and 4D). In contrast to the PLGA/PEI-pCAIX immunization group, PLGA/PEI-pFGL1/pCAIX co-immunization group also showed a remarkable increase of the level of IFN-γ-secreted by T lymphocytes (Figures 4E and 4F). Moreover, the proportion of tumor necrosis factor (TNF)-α^+CD8$^+$, IL-2$^+$CD8$^+$, and IFN-γ^+CD8$^+$ T cells in the PLGA/PEI-pFGL1/pCAIX co-immunization group was significantly higher than that in PLGA/PEI-pCAIX alone immunization group (Figures 4G and 4H), indicating that PLGA/PEI-pFGL1/pCAIX vaccine could enhance the induction of functional CD8$^+$ T cells. These results suggest that PLGA/PEI-pFGL1/pCAIX vaccine greatly enhances tumor antigen-specific CD8$^+$ T cell immune responses.

Multi-functional CD8$^+$ T cells are required for the anti-tumor effect of PLGA/PEI-pFGL1/pCAIX nano-vaccine

The protective immunity against tumor can be performed by multi-functional CD8$^+$ T cells that secrete multiple cytokines (TNF-α, IL-2, and IFN-γ), which are considered to be the key effector cells of the immune system.[27] Therefore, PLGA/PEI-pFGL1/pCAIX vaccine-induced specific multi-functional CD8$^+$ T cells were tested in

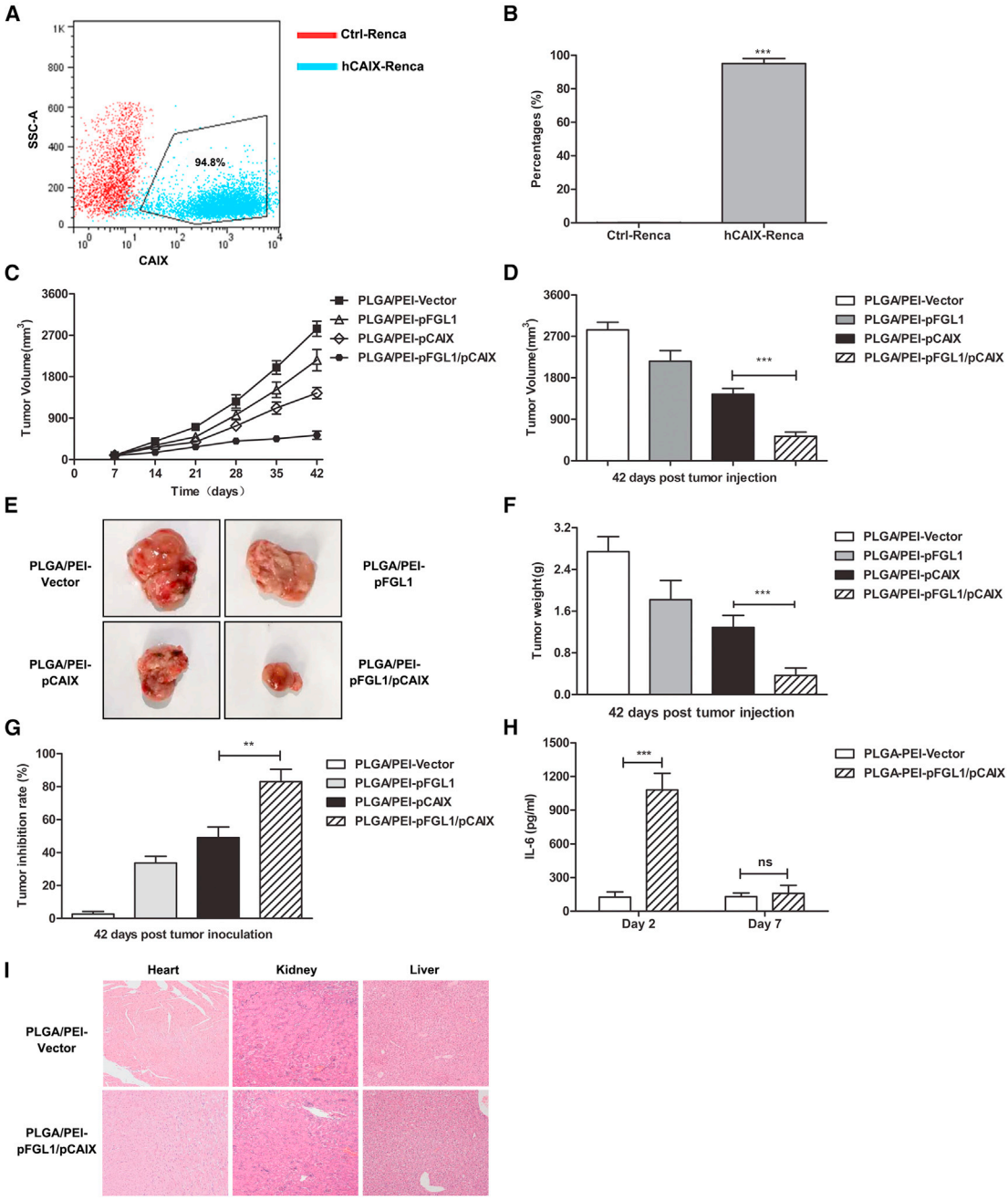

Figure 2. Therapeutic effects of PLGA/PEI-pFGL1/pCAIX vaccine in subcutaneous hCAIX-Renca tumor model

(A and B) The percentage of CAIX expression was determined by flow cytometry in Renca cells infected with hCAIX-lentivirus. BALB/c mice were inoculated subcutaneously at the right flank with 2×10^5 hCAIX-Renca cells. Seven days later, mice were intramuscularly inoculated with various vaccines. (C) Tumor progression was evaluated by measurement of tumor volume once every 7 days from day 0 to day 42. (D) Forty-two days after tumor inoculation, tumor volumes were measured. (E) One representative picture of resected tumors was shown per group. (F) Tumor weights. (G) Tumor inhibition rate. (H) The levels of IL-6 were detected by ELISA in the serum of the mice treated with PLGA/PEI-Vector or PLGA/PEI-pFGL1/pCAIX. (I) Mice were sacrificed on day 42 after tumor inoculation, and the pathology was evaluated by H&E staining of heart, kidney, or liver tissues. Each experiment was performed independently at least three times and the results of one representative experiment are shown. Data are means ± SD, $^{**}p < 0.01$ and $^{***}p < 0.001$; ns, no significant difference.

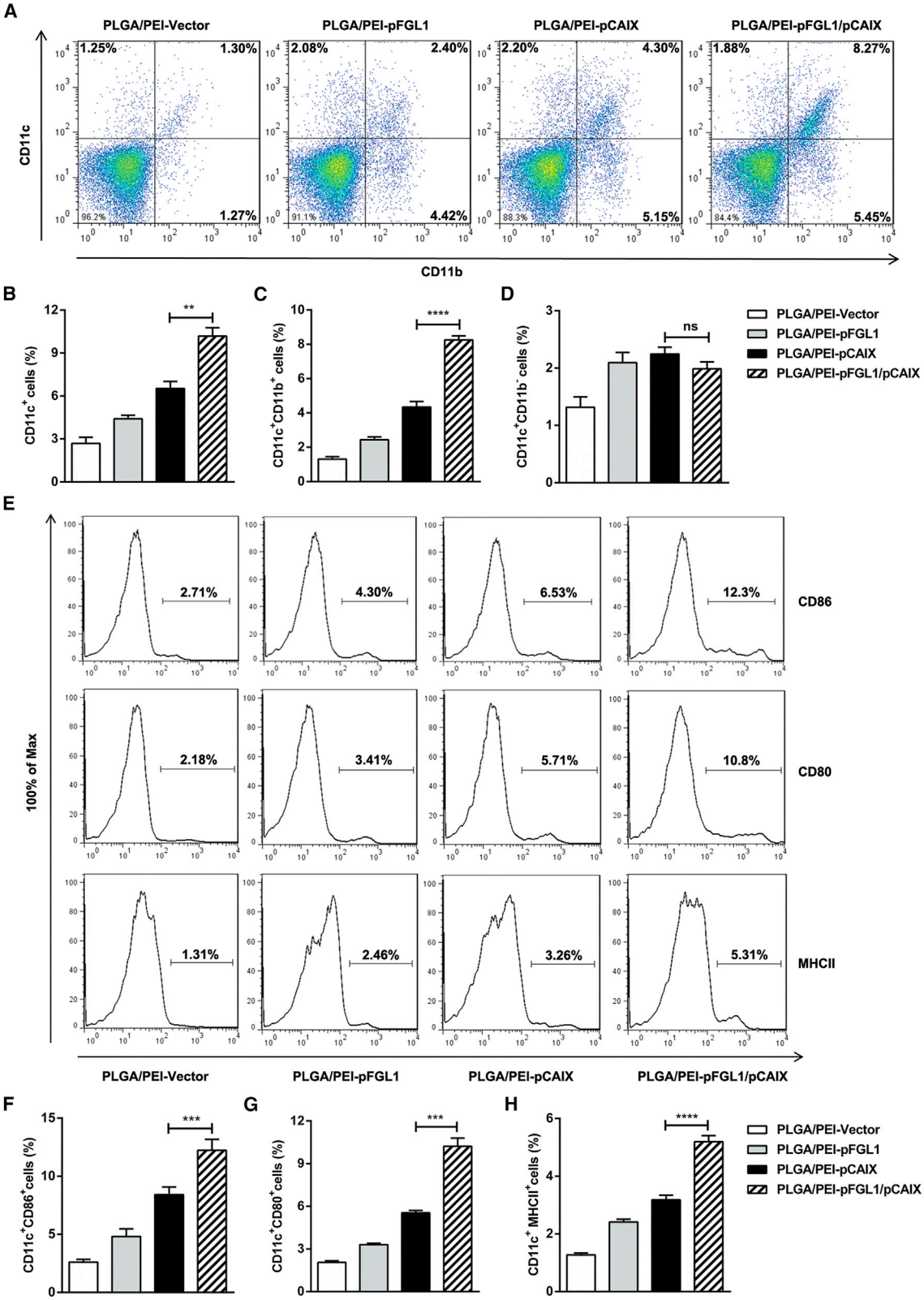

(legend on next page)

spleen and tumor-infiltrating leukocytes (TIL) of mice. Flow cytometry results showed that the percentages and number of TNF-α^+IL-2$^+$CD8$^+$, TNF-α^+IFN-γ^+CD8$^+$, IL-2$^+$IFN-γ^+CD8$^+$, and TNF-α^+IL-2$^+$IFN-γ^+CD8$^+$ T cells were significantly increased in spleen (Figures 5A and 5B) and TIL (Figures 5C and 5D) of PLGA/PEI-pFGL1/pCAIX group compared with PLGA/PEI-pCAIX group. These data implied that PLGA/PEI-pFGL1/pCAIX vaccine effectively enhanced the induction of antigen-specific multi-functional CD8$^+$ T cells. To determine whether multi-functional CD8$^+$ T cells were critical for the anti-tumor activity induced by the vaccine, we used the CD8 mAb to eliminate CD8$^+$ T cells in tumor-bearing mice immunized with PLGA/PEI-pFGL1/pCAIX vaccine. Administration of CD8 mAb resulted in the significantly reduced percentages of CD8$^+$ T cells in spleen or TIL from PLGA/PEI-pFGL1/pCAIX-treated mice, indicating that the CD8$^+$ T cells could be effectively deleted *in vivo* (Figure 5E). Accordingly, the tumor growth of PLGA/PEI-pFGL1/pCAIX co-immunized mice was uncontrolled after depleting CD8$^+$ T cells (Figures 5F and 5G). Likewise, the reduced tumor inhibition rate was observed in CD8 mAb-treated mice immunized with PLGA/PEI-pFGL1/pCAIX vaccine (Figure 5H). These results suggest that multi-functional CD8 T cell responses play a key role for the anti-tumor effect of PLGA/PEI-pFGL1/pCAIX vaccine.

PLGA/PEI-pFGL1/pCAIX vaccine exerts a potent therapeutic effect in the mouse lung metastasis model

To evaluate the therapeutic effect of PLGA/PEI-pFGL1/pCAIX vaccine for metastatic tumor, a mouse model of lung metastasis was established. The vaccine-treated mice were sacrificed on day 28 post tumor inoculation, and the lungs were surgically removed and the visible metastases were counted. As shown in Figures 6A and 6B, a significantly reduced number of lung metastases was observed in PLGA/PEI-pFGL1/pCAIX vaccine-treated mice compared with PLGA/PEI-pCAIX vaccine-treated mice. The protective effect of PLGA/PEI-pFGL1/pCAIX vaccine was further confirmed by H&E staining results of lung tissues (Figures 6C and 6D). Moreover, the infiltration of CD8$^+$ T cells was detected by immunohistochemistry (IHC) experiments in the lung tissues from mice immunized with various vaccines. The number of brownish yellow particles (CD8$^+$ T cells) was significantly increased in the lung tissue sections of mice immunized with PLGA/PEI-pFGL1/pCAIX vaccine in contrast to PLGA/PEI-pCAIX vaccine (Figure 6E). Likewise, we also measured the infiltration of CD8$^+$ T cells by flow cytometry in lung tissues and found that the percentage of CD8$^+$ T cells was significantly higher in PLGA/PEI-pFGL1/pCAIX co-immunization group (Figure 6F). These results indicate that PLGA/PEI-pFGL1/pCAIX vaccine could effectively inhibit the tumor lung metastasis of renal cancer.

Furthermore, multi-functional CD8$^+$ T cell responses were analyzed *in vitro*. The cell proliferation assay showed that a remarkably increased percentage of CD8$^+$ T cells was observed in antigen-treated lymphocytes from PLGA/PEI-pFGL1/pCAIX-immunized mice as compared with control mice (Figure 6G). The PLGA/PEI-pFGL1/pCAIX group also promoted the number of IFN-γ-secreting T cells demonstrated by ELISPOT assay (Figure 6H). Accordingly, the percentages of the multi-functional CD8 T cells were evaluated by flow cytometry, and the strongest increase was seen in the PLGA/PEI-pFGL1/pCAIX co-immunization group compared with the other immunization group (Figure 6I). Moreover, the effector cells from PLGA/PEI-pFGL1/pCAIX co-immunized mice also showed a stronger CTL effect against hCAIX-Renca cells (Figure 6J). Together, these results indicate that FGL1 combined with CAIX-based vaccine synergistically enhances the induction of multi-functional CD8$^+$ T cell responses and prevents the tumor growth of lung metastasis in renal cancer.

DISCUSSION

Tumor DNA vaccines can provide a potential option for cancer immunotherapy by inducing antigen-specific T cell immune responses.[36] CAIX as a tumor-specific antigen is an ideal target for the immunotherapy of renal caner, but the immunogenicity of alone CAIX is too weak to activate the lasting and effective immune responses.[37] Therefore, co-immunization with adjuvant or other tumor antigen is need for effectively improving DNA vaccine immunogenicity and causing a strong immune response. FGL1 is considered as an immune inhibitory ligand of LAG-3 or a tumor antigen, thus targeting FGL1 in the tumor microenvironment can enhance T cell immunity and inhibit tumor growth.[32] Therefore, the designed dual FGL1/CAIX vaccine might induce humoral immunity to block the interaction between FGL1-LAG-3 and enhance tumor antigen-specific T cell responses. Our results demonstrated that FGL1 combined with CAIX vaccine could effectively inhibit the tumor growth in the mouse subcutaneous tumor model and lung metastasis model.

The delivery system is another key factor that affects the efficacy of tumor DNA vaccines.[38] In recent years, biodegradable PLGA has become one of the most representative nanostructure materials and is approved for use in biomedical systems.[39] PEI is a cationic material with a high stability, is easy to handle and bind to DNA, and is a commonly used material for gene delivery.[40,41] PLGA conjugated to PEI for gene delivery can avoid PEI-induced cytotoxicity by excessive positive charge and the aggregation on the cell surface.[42] PLGA/PEI-based polyplexes have been shown to be an effective transfection agent for DNA vaccine delivery.[43] Our results also showed that PLGA/PEI-pFGL1/CAIX nano-vaccine could be efficiently expressed

Figure 3. The induction and maturation of DCs by PLGA/PEI-pFGL1/pCAIX nano-vaccine in mice

(A) Mice immunized with vaccines were sacrificed at 42 days post tumor inoculation, and the proportions of CD11c$^+$ or CD11c$^+$CD11b$^+$ cells were analyzed by flow cytometry in spleen. One representative flow cytometry result was shown for per group. (B–D) Statistical analysis of the frequencies of CD11c$^+$, CD11c$^+$CD11b$^+$, or CD11c$^+$CD11b$^-$ cells in (A). (E) The expression of CD86, CD80, or MHCII on CD11c$^+$ cells. (F–H) Statistical analysis of the frequencies of CD11c$^+$CD86$^+$, CD11c$^+$CD80$^+$, or CD11c$^+$MHCII$^+$ cells in (E). The data shown are representative of three experiments. Data are means ± SD. The different significance was set at $^*p < 0.05$, $^{**}p < 0.01$, $^{***}p < 0.001$.

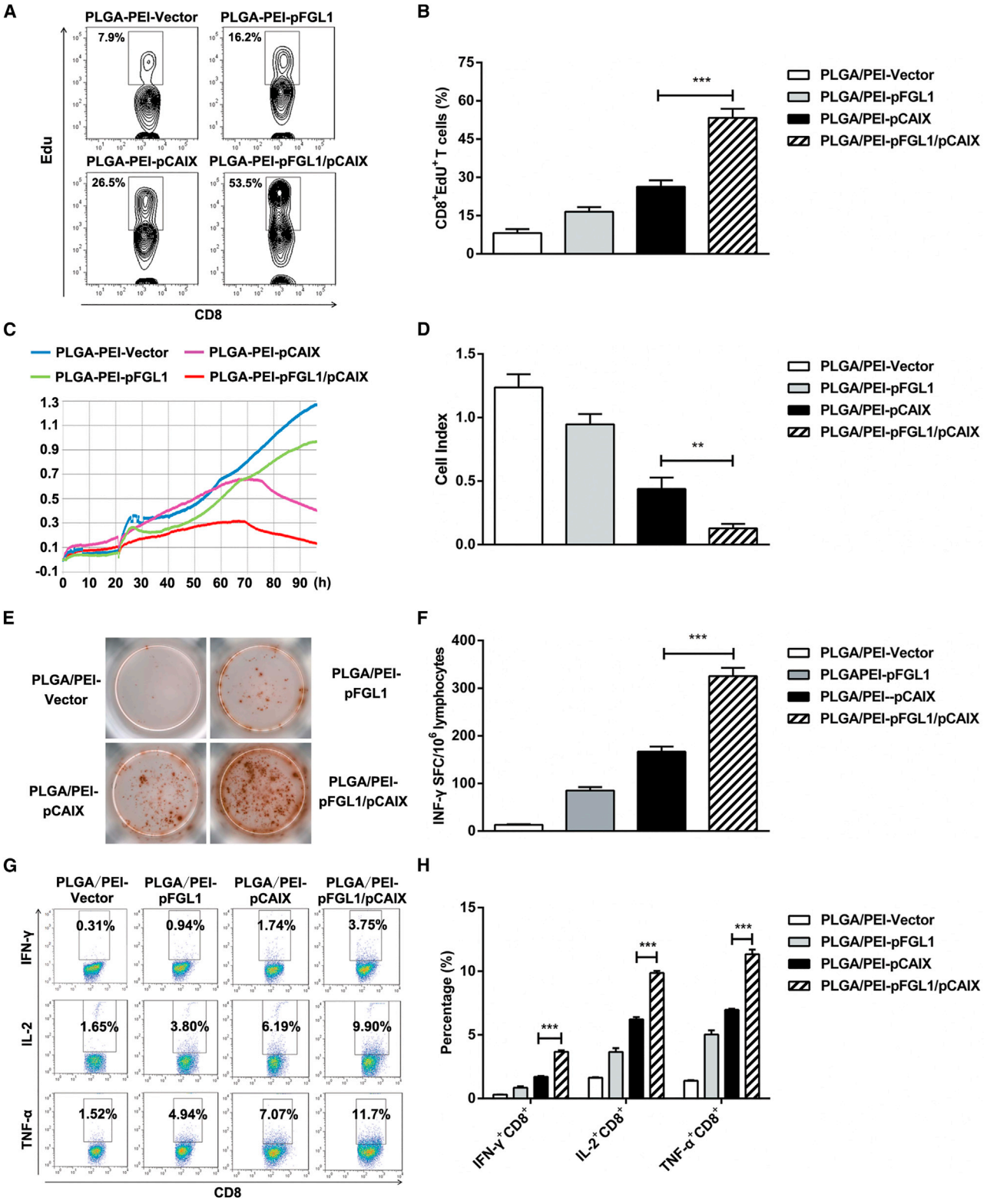

(legend on next page)

in vitro or *in vivo*. Therefore, PLGA/PEI-based delivery system can promote DNA vaccine expression and therapeutic effect.

The induction or recruitment of mature $CD11c^+$ DCs is essential for antigen presentation and induction of tumor-specific $CD8^+$ T cells to exert durable protective immunity.[44] In tumor models treated with chemotherapy, mature $CD11b^+CD11c^+$ DC subset is an important class of antigen-presenting cells for optimal immune system-mediated anti-tumor responses.[45] Moreover, the $CD11b^+CD11c^+$ myeloid cells can enhance the induction of inducible nitric oxide synthase (iNOS) in tumor cells and promote tumor cell apoptosis.[46] Therefore, the induction of $CD11b^+CD11c^+$ DCs is beneficial to improve the therapeutic efficacy of DNA vaccines. In this study, PLGA/PEI-pFGL1/pCAIX co-immunization significantly increased the proportion of $CD11c^+$ DCs and $CD11b^+CD11c^+$ DC subsets, and at the same time increased the expression of CD80, CD86, or MHCII. These results indicated that the PLGA/PEI-pFGL1/pCAIX vaccine could induce the increase of DCs *in vivo* and promote their maturation.

The functional $CD8^+$ T cells are the main anti-cancer effector cells in the cancer microenvironment.[47] However, the intratumoral $CD8^+$ T cells are usually in a state of dysfunction, which suppresses cell proliferation and activation and impairs anti-cancer effects. PLGA/PEI-pFGL1/pCAIX vaccine co-immunization significantly promoted the $CD8^+$ T cell proliferation, CTL responses, and multi-functional $CD8^+$ T cell immune responses, indicating that this vaccine could effectively improve the function of intratumoral $CD8^+$ cells and activate the body's immune system. In order to further verify the important role of $CD8^+$ T cells induced by PLGA/PEI-pFGL1/pCAIX vaccine for renal cancer treatment, we used mAbs to delete $CD8^+$ T cells, and the results showed that PLGA/PEI-pFGL1/pCAIX treatment with $CD8^+$ T cell deletions has no obvious therapeutic effect. These results indicated that the therapeutic function of the PLGA/PEI-pFGL1/pCAIX vaccine mainly depends on the $CD8^+$ T cell-mediated immune responses.

In summary, we designed a DNA vaccine containing dual targets of FGL1 and CAIX, and the vaccine was delivered by PLGA/PEI nanoparticle delivery system. Our results showed that FGL1 can be used as an immune adjuvant or antigen to enhance the immunogenicity of CAIX antigen, thereby inducing the maturation of DCs in the body and further promoting the multi-functional $CD8^+$ T cell-mediated immune responses. Accordingly, PLGA/PEI-pFGL1/pCAIX vaccine effectively suppressed the tumor development in subcutaneous and lung metastatic models of renal cancer. This vaccine strategy might provide a new way for the immunotherapy of kidney cancer and lay the experimental foundation for other solid tumors.

MATERIALS AND METHODS

Construction of eukaryotic expression plasmids of pCAIX or pFGL1

The full-length mouse FGL1 (mFGL1) cDNA sequence was amplified by PCR using the template pECMV-FGL1-m-FLAG vector (Miaoling Bio, Wuhan, China). The amplified DNA fragments were separated by standard gel electrophoresis and then purified by using AxyPrep DNA Gel Extraction Kit (Axygen) according to the manufacturer's instructions. The gel extraction PCR fragment then was subcloned into the Hind III and Xba I sites of pcDNA3.1 vector to obtain the plasmid FGL1 (pFGL1). The pFGL1 was sequenced to confirm that it was successfully constructed. The human CAIX (hCAIX) plasmid pcDNA3.1-CAIX (pCAIX) has been constructed previously.[27] pFGL1 or pCAIX were transformed into DH5a bacteria competent cells, propagated in LB broth supplemented with 100 μg/mL ampicillin, and purified from the bacteria grown overnight by using Endo-Free Plasmid Mega kit (Qiagen) according to the manufacturer's instruction.

Preparation of vaccines

Poly(lactic-co-glycolic acid) (PLGA) nanoparticles are prepared by a modified water-in-oil-in-water emulsion-solvent evaporation (W/O/W) double emulsion-solvent evaporation method.[48] Briefly, 100 mg PLGA (MedChem Express) was added to 1 mL dichloromethane by sonication for 30 s. Next, 3 mL of polyvinyl alcohol (PVA) solution (7%, w/v) was added to the W/O single emulsion before being tip-sonicated for 10 min. Then the above solution was dripped into 50 mL of PVA solution (1%, w/v) containing 2% isopropanol and then maintained under mechanical stirring for 1 h at 600 rpm. After centrifugation at 8,000 × *g* for 40 min, purified PLGA nanoparticles were obtained. The above particles were washed twice, paying attention to avoid agglomeration of particles.

Next, PEI (branched, 25 kDa; Sigma) solution (2 mg/mL) was mixed with PLGA solution (1.5 mg/mL) and then soft vortexing for 15 s. The aforesaid mixture was kept at room temperature (RT) for at least 1 h. After preparation of the PLGA/PEI complex, plasmid DNA solution (1 mg/mL) was mixed with polycation nanoparticles and then soft vortexed for 1 min. The prepared PLGA/PEI/pDNA polyplexes were characterized by their size and zeta-potential with the Zeta sizer Nano ZS (Malvern, Southborough, MA). The nanoparticle vaccines were stabilized for 30 min at RT prior to immunization.

Cell lines and cell culture

The human HEK293T cell line and murine renal cancer Renca cell line used in the experiment were obtained from the American Type Culture Collection and Cobioer Biosciences (Nanjing, China), respectively, and passed the certificate of analysis. In a 5% CO_2 atmosphere at 37°C,

Figure 4. CD8 T cell responses induced by PLGA/PEI-pFGL1/pCAIX co-immunization

(A and B) The lymphocytes isolated from spleen of immunized mice were stimulated with CAIX protein (10 μg/mL) *in vitro*; the percentages of EdU^+ cells were assessed in gated CD8 T cells by flow cytometry. (C and D) RTCA assay was used to measure the CTL activity. (E and F) IFN-γ-secreting T lymphocytes were detected by ELISPOT assay. (G and H) Flow cytometry was performed to assess the proportion of TNF-α^+CD8^+, IL-2^+CD8^+, and IFN-γ^+CD8^+ T cells in the stimulated splenocytes. Experiments were individually conducted thrice; one representative experiment is shown as results for each group of mice. Data are means ± SD. $^{**}p < 0.01$, $^{***}p < 0.001$.

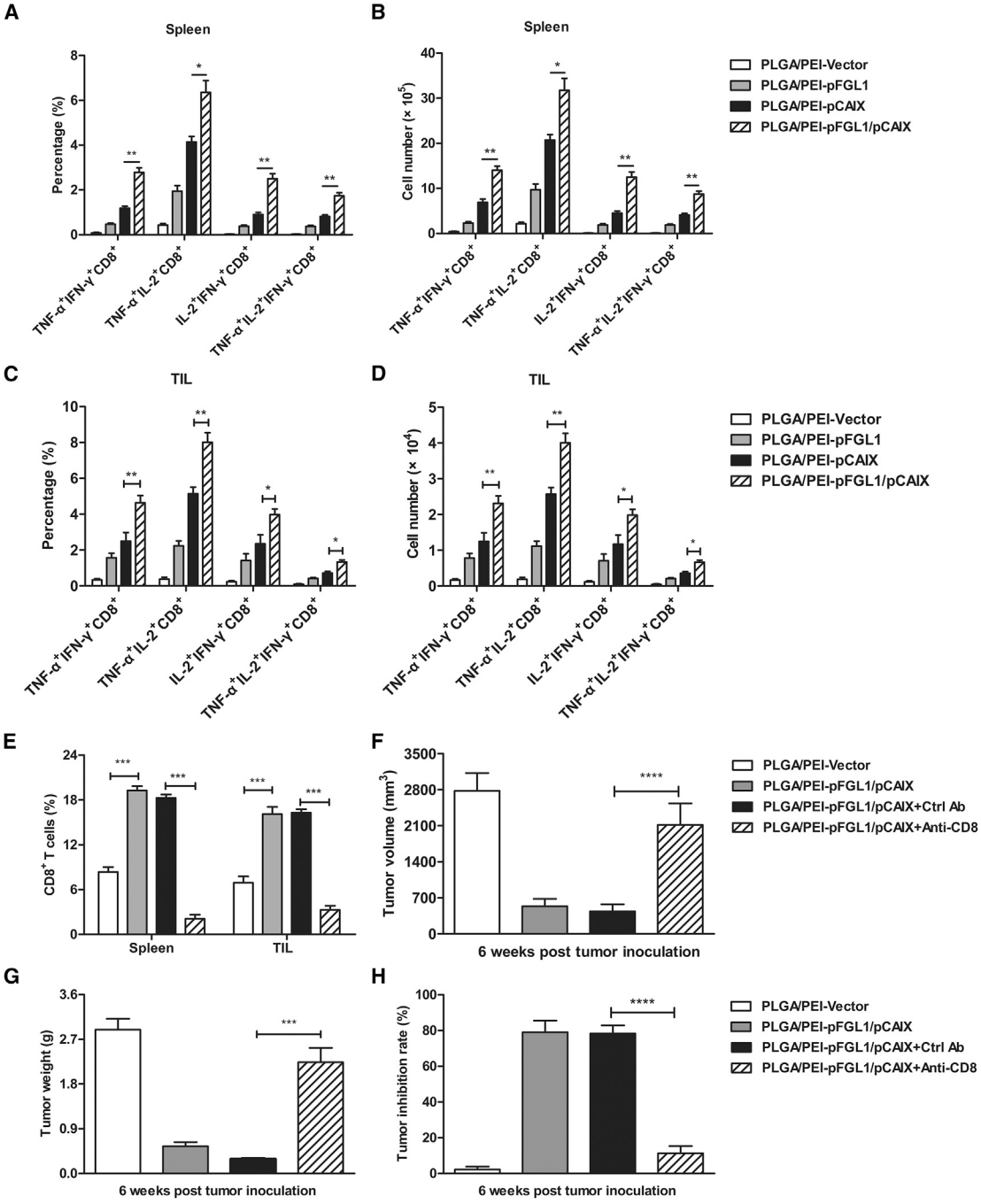

Figure 5. The anti-tumor effect induced by PLGA/PEI-pFGL1/pCAIX vaccine was dependent on multi-functional CD8$^+$ T cell responses

Forty-two days after tumor inoculation, splenocytes from vaccine-immunized mice were stimulated with 10 μg/mL CAIX protein at 37°C and 5% CO_2 for 3 days, then 500 ng/mL Ionomycin, 50 ng/mL PMA, and 5 ng/mL Brefeldin A were added to incubate for 5 h *in vitro*. (A and B) The proportions and number of tumor-specific CD8$^+$ T cells expressing two or three markers of TNF-α, IL-2, and IFN-γ were detected by flow cytometry in the stimulated splenocytes. (C and D) The proportions and number of tumor-specific TNF-α$^+$IL-2$^+$CD8$^+$, TNF-α$^+$IFN-γ$^+$CD8$^+$, or TNF-α$^+$IL-2$^+$IFN-γ$^+$CD8$^+$ T cells in the TIL of tumors. In the depleted group of mice, 0.5 mg of anti-mouse CD8 mAb was injected intraperitoneally at days −2, 5, and 12 after vaccination. (E) The proportions of CD8$^+$ T cells in spleen or TIL from PLGA/PEI-pFGL1/pCAIX vaccine-immunized tumor-bearing mice treated with or without CD8 mAb. (F) Tumor volumes on day 42 post tumor inoculation. (G) Tumor weights. (H) Tumor inhibition rate. Experiments were individually conducted thrice; one representative experiment is shown as results for each group of mice. Data are means ± SD. *$p < 0.05$, **$p < 0.01$, ***$p < 0.001$, ***$p < 0.0001$.

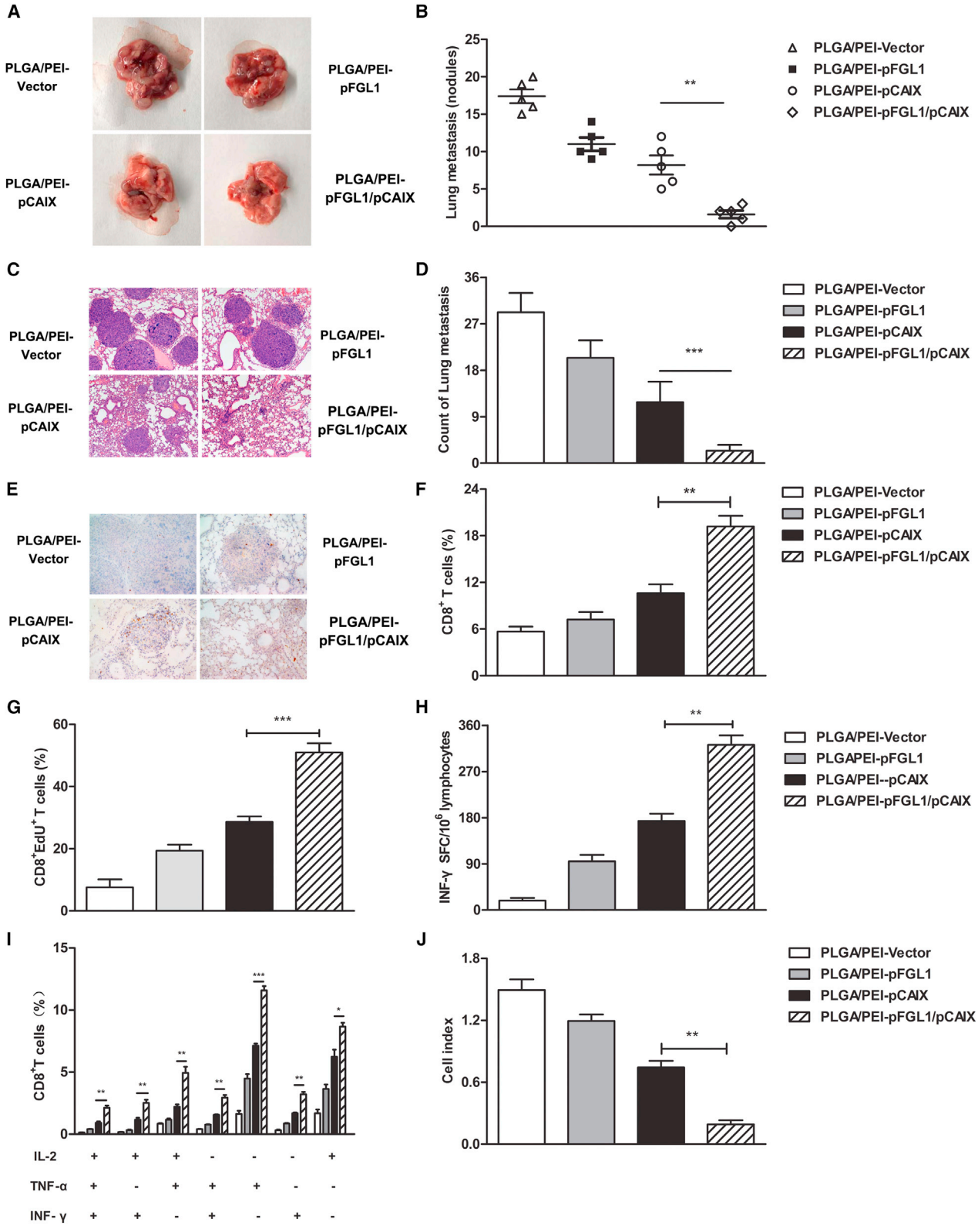

(legend on next page)

HEK293T cells were cultured in DMEM medium (Gibco, Invitrogen) containing 10% fetal bovine serum (FBS) (ExCell Bio), 100 U/mL penicillin (Sangon Biotech), and 100 μg/mL streptomycin (Sangon Biotech). Renca cells were supplemented with 10% FBS, 100 U/mL penicillin, 100 μg/mL streptomycin, 2 mM L-glutamine (Sigma), 1 × MEM non-essential amino acid solution (Sigma), and 1 mM sodium pyruvate solution (Sigma) in RPMI 1640 medium (Gibco, Invitrogen). All cells cultured in medium were passaged for less than 6 weeks before renewing from a frozen, early passaged population. The stable overexpressing hCAIX-Renca cells were established by Renca cells infected with CAIX lentivirus produced by HEK293T cells.

Western blot

The equal amounts of proteins solubilized in the SDS sample buffer were separated by 10% SDS-PAGE, transferred to polyvinylidene difluoride (PVDF) membranes, and incubated with appropriate dilutions of primary antibodies against mFGL1 (ProteinTech, Wuhan, China), hCAIX (Abcam), and GAPDH (Cell Signaling Technology) overnight at 4°C. After washing with Tris-buffered saline containing 0.1% tween 20 (TBST), the membranes were incubated with horseradish peroxidase (HRP)-linked secondary antibody (Southern Biotech, Birmingham, AL) for 2 h at RT and rinsed with TBST. Then, the immunoreactive bands were detected by chemiluminescence using the ECL (Thermo Fisher Scientific).

Animal model and vaccine immunization

Female BALB/c mice (6 weeks old) were purchased from Vital River Laboratory (Beijing, China) and fed under specific-pathogen-free conditions. All animal procedures and protocols were approved by the Experimental Animal Ethics Committee of Xuzhou Medical University, and implemented in accordance with the Xuzhou Medical University Laboratory Animal Care and Use Guide.

For the subcutaneous tumor model, mice were subcutaneously inoculated with hCAIX-Renca cells (2×10^5 cells/mouse). Tumor-bearing mice were immunized with PLGA/PEI-vector, PLGA/PEI-pFGL1, PLGA/PEI-pCAIX, and PLGA/PEI-pFGL1/pCAIX at a dose of 50 μg each plasmid. The vaccines were used for re-vaccinated mice on the 10th and 20th days after the initial vaccination. Tumor volume was evaluated once a week based on the formula V (mm^3) = (length × $width^2$)/2. The tumor tissues were taken out and weighed after the mice were killed. The tumor inhibition rates were calculated using the following equation: Tumor inhibition rate (%) = $(1-W_{sample}/W_{control}) \times 100\%$. $W_{control}$ and W_{sample} represented the weight of tumors in the control and sample groups at the end of the experiment, respectively. The major organs were removed for histological examination by H&E staining.

For the lung metastasis tumor models, 10 days after intramuscular injection of each vaccine, mice were injected intravenously with 5×10^5 hCAIX-Renca cells/mouse into the lungs, and then the vaccines were re-inoculated to boost immune responses on the 10th and 20th day post tumor cell inoculation. At day 28 after tumor inoculation, mice were sacrificed, and the lungs were removed and the metastatic nodules counted.

Separation of splenocytes and TIL

Splenocytes were prepared by gently homogenizing the tissues to release the cells. Debris was removed by filtering through a 70-mm nylon mesh, and then red blood cells were lysed with ACK lysis buffer. Tumor tissues were dissected into smaller pieces and digested before being homogenized through 70-mm mesh cell strainers to generate single-cell suspensions. TIL was prepared by processing the tissues into single-cell suspensions, and leukocytes were separated on a 33% Percoll (VicMed) gradient. Red blood cells were lysed.

Flow cytometry analysis

For cell surface staining, cells were incubated with anti-mouse FITC-CD11b (Biolegend), APC-CD11c (Biolegend), PE-CD80 (Biolegend), PE-CD86 (Biolegend), and PE-MHCII (Biolegend) after FcR blocking. Isotype-matched mouse immunoglobulin served as control. For intracellular cytokine staining, splenocytes were plated into a 12-well culture plate at a density of 4×10^6/mL and stimulated with 10 μg/mL CAIX protein at 37°C and 5% CO_2 for 72 h. These cells were also stimulated with 500 ng/mL Ionomycin (Sigma-Aldrich) and 50 ng/mL PMA (Sigma-Aldrich) plus 5 ng/mL Brefeldin A (BFA, eBioscience) for the last 5 h. Cell surface staining was performed on the stimulated splenocytes or isolated TILs with anti-mouse PerCP-Cy5.5-CD8α (BD Pharmingen), and then intracellular staining was performed with anti-mouse APC-IFN-γ (BD Pharmingen), PE-IL-2 (BD Pharmingen), and FITC-TNF-α (BD Pharmingen). FlowJo software (Tree Star Inc) analyzed the sample data acquired from BD FACSCanto II (BD Biosciences) in FACSDiva software (BD Biosciences).

Proliferation assay of CD8 T cells

Splenocytes were added into 48-well flat-bottomed tissue culture plates at 1×10^6 cells/well containing IL-2 (50 U/mL) and CAIX

Figure 6. PLGA/PEI-pFGL1/pCAIX vaccine-induced multi-functional $CD8^+$ T cell responses and suppressed the lung metastasis of renal cancer model

(A) The present images of lung metastasis tumors excised from mice. (B) The numbers of metastatic nodules were quantified in the lung tissue sections of the tumor-bearing mice. (C) Lung tissues performed by H&E staining. (D) The count of lung metastasis in (C). (E) $CD8^+$ T cells of lung tissues from metastatic tumor mice were detected by immunochemistry staining on day 28 (×200 magnification). (F) At day 28 post tumor inoculation, mice were killed and the frequencies of $CD8^+$ T cells were analyzed by flow cytometry in the lungs in various vaccine groups. (G) CD8 T cell proliferation was detected by flow cytometry according to EdU assay. (H) CAIX-specific IFN-γ-secreting T lymphocyte cells were quantified by ELISPOT assay. (I) Intracellular staining of TNF-α, IFN-γ, and IL-2 of multi-functional $CD8^+$ T cells in stimulated splenocytes. (J) The CTL effect of splenocytes from tumor mice immunized with various vaccines against hCAIX-Renca cells were detected by RTCA assay; cell indexes were analyzed. The experiments were performed with five mice per group. Data are from one representative experiment of three performed and presented as the mean ± SD. The different significance was set at $^{**}p < 0.01$, $^{***}p < 0.001$.

antigen protein (10 μg/mL). The plates were cultured at 37°C in a humidified incubator with 5% CO_2 for 5 days and the medium was changed at 3 days. Cell proliferation assay was performed using the BeyoClick EdU Cell Proliferation Kit with Alexa Fluor 647 (Beyotime). Briefly, the cells were incubated with 10 μM EdU for 2 h at 37°C. Then, cells were collected and surface staining was performed with PerCP-Cy5.5-CD8α for 30 min. After fixation, permeabilization, and rinse, the cells were exposed to 100 μL of click reaction cocktail for 30 min. The cells were washed three times with permeabilization buffer. The percentages of EdU^+ cells in $CD8^+$ T cells were analyzed by flow cytometry and defined as the proliferation rate.

RTCA killing test

Splenocytes were cultured in RPMI 1640 medium containing 50 U/mL IL-2 and 10 μg/mL CAIX protein for 7 d at 37°C in humidified air with 5% CO_2. The processed cells were washed and resuspended as effector cells in RPMI 1640. hCAIX-Renca were used as target cells. Complete medium was added to RTCA plate (ACEA Biosciences. Inc) at 50 μL/well and then the baseline was measures. Target cells were resuspended in complete medium at 10^4 cells/well. After the cells adhered, effector cells were added by the effector-target cell ratio of 50:1 and incubated for 96 h. Finally, RTCA analysis software (ACEA Biosciences. Inc) was used to analyze the data.

ELISPOT assay

The splenocytes from immunized mice were isolated and plated (1×10^6 cells/well) in an enzyme-linked immunosorbent spot (ELISPOT) 96-well plate (Millipore) coated with the IFN-γ capture antibody (eBioscience), and then stimulated with CAIX protein (10 μg/mL) for 60 h at 37°C with 5% CO_2. After sequential incubation with biotinylated detection antibody, streptavidin-HRP, and AP-colorimetric substrate (eBioscience), color was developed and spot-forming cells were counted using an ELISPOT reader system (AID).

Depletion of CD8 T cells

To deplete CD8 T cells *in vivo*, mice received intraperitoneal injections of 0.5 mg purified anti-mouse CD8 mAb (clone 53-6.7) 2 days before administration of vaccines in the therapeutic model, and then the antibody injections were repeated on day 5 and day 12 after the first vaccination. The efficacy of cell depletion was confirmed by flow cytometric analysis of the spleens.

IHC staining

The paraffin tissue sections were initially deparaffinized at 65°C for 1 h, placed in xylene solutions I and II for further permeabilization for 5 min, and then dehydrated in gradient dilution of alcohol solution. Subsequently, epitopes of rehydrated sections were retrieved by a heat-induced protocol. The sections were blocked with 10% BSA and incubated with anti-mouse CD8 antibody (eBioscience) at 4°C overnight. After washing with PBS, the sections were stained with an IHC kit (Zhongshan Biotechnology Co., Ltd., Beijing) according to the manufacturer's instructions. Pictures of stained sections were taken on a Nikon SCLIPSS TE2000-S microscope (Nikon) equipped with ACT-1 software at ×200 magnification.

Pathological analyses

Lung tissues from mice were removed, fixed with 4% paraformaldehyde, embedded in paraffin, cut into 5 μm slices, H&E stained according to the manufacturer's instructions, and blinded by different pathologists to evaluate histopathological sections. Then photos were taken on a Nikon SCLIPSS TE2000-S microscope (Nikon) equipped with ACT-1 software at ×200 magnification.

Statistical analyses

Statistical significance was evaluated with GraphPad Prism Software (Version 6.01). Comparison of two groups was analyzed using two-tailed Student t test and multiple comparisons were performed using one-way ANOVA. Data were presented as means ± SD. The statistical p value was set as $^*p < 0.05$; $^{**}p < 0.01$; and $^{***}p < 0.001$ for different significance levels.

ACKNOWLEDGMENTS

This project was supported by grants from the National Natural Science Foundation of China (No. 82072814), Jiangsu Province Natural Science Foundation (BK20190986), Key Research Development project of Xuzhou (Industry Foresight and Common Key Technology) (No. KC19082), Key R&D and Promotion Project in Henan Province (212102310751), Scientific Studio of Zhongyuan Scholars (214400510018), Qing Lan Project of Jiangsu Province, and the Youth Technology Innovation Team of Xuzhou Medical University (TD202003).

AUTHOR CONTRIBUTIONS

D.C., G.W., and J.Z. conceived and designed the project. D.C., D.Q., J.D., Z.C., N.J., and J.W. performed the project. D.C., Z.C., D.Q., J.D., N.J., and P.X. analyzed the data. G.W., J.Y., and J.Z. contributed reagents/materials/analysis tools. D.C. and D.Q. wrote the paper. All authors read and approved the final manuscript.

DECLARATION OF INTERESTS

The authors declare no conflict of interest.

REFERENCES

1. Lindblad, P. (2004). Epidemiology of renal cell carcinoma. Scand. J. Surg. *93*, 88–96.
2. Bray, F., Ferlay, J., Soerjomataram, I., Siegel, R.L., Torre, L.A., and Jemal, A. (2018). Global cancer statistics 2018: GLOBOCAN estimates of incidence and mortality worldwide for 36 cancers in 185 countries. CA: Cancer J. Clin. *68*, 394–424.
3. Gupta, K., Miller, J.D., Li, J.Z., Russell, M.W., and Charbonneau, C. (2008). Epidemiologic and socioeconomic burden of metastatic renal cell carcinoma (mRCC): a literature review. Cancer Treat. Rev. *34*, 193–205.
4. Ljungberg, B., Cowan, N.C., Hanbury, D.C., Hora, M., Kuczyk, M.A., Merseburger, A.S., Patard, J.J., Mulders, P.F.A., and Sinescu, I.C. (2010). European Association of Urology Guideline Group. EAU guidelines on renal cell carcinoma: the 2010 update. Eur. Urol. *58*, 398–406.
5. Posadas, E.M., Limvorasak, S., and Figlin, R.A. (2017). Targeted therapies for renal cell carcinoma. Nat. Rev. *13*, 496–511.
6. Bindayi, A., Hamilton, Z.A., McDonald, M.L., Yim, K., Millard, F., McKay, R.R., Campbell, S.C., Rini, B.I., and Derweesh, I.H. (2018). Neoadjuvant therapy for localized and locally advanced renal cell carcinoma. Urol. Oncol. *36*, 31–37.
7. Kim, S.H., Park, B., Hwang, E.C., Hong, S.H., Jeong, C.W., Kwak, C., Byun, S.S., and Chung, J. (2019). Retrospective multicenter long-term follow-up analysis of prognostic

risk factors for recurrence-free, metastasis-free, cancer-specific, and overall survival after curative nephrectomy in non-metastatic renal cell carcinoma. Front. Oncol. *9*, 859.

8. Bluthgen, M.V., Baste, N., and Recondo, G. (2020). Immunotherapy combinations for the treatment of patients with solid tumors. Future Oncol. *16*, 1715–1736.
9. Keilson, J.M., Knochelmann, H.M., Paulos, C.M., Kudchadkar, R.R., and Lowe, M.C. (2021). The evolving landscape of immunotherapy in solid tumors. J. Surg. Oncol. *123*, 798–806.
10. Orr, M.T., Khandhar, A.P., Seydoux, E., Liang, H., Gage, E., Mikasa, T., Beebe, E.L., Rintala, N.D., Persson, K.H., Ahniyaz, A., et al. (2019). Reprogramming the adjuvant properties of aluminum oxyhydroxide with nanoparticle technology. NPJ Vaccin *4*, 1–10.
11. Melief, C.J., van Hall, T., Arens, R., Ossendorp, F., and van der Burg, S.H. (2015). Therapeutic cancer vaccines. J. Clin. Invest. *125*, 3401–3412.
12. Sarkar, I., Garg, R., and van Drunen Littel-van den Hurk, S. (2019). Selection of adjuvants for vaccines targeting specific pathogens. Expet Rev. Vaccin. *18*, 505–521.
13. Seya, T., Shime, H., Takeda, Y., Tatematsu, M., Takashima, K., and Matsumoto, M. (2015). Adjuvant for vaccine immunotherapy of cancer–focusing on Toll-like receptor 2 and 3 agonists for safely enhancing antitumor immunity. Cancer Sci. *106*, 1659–1668.
14. Pastorek, J., and Pastorekova, S. (2015). Hypoxia-induced carbonic anhydrase IX as a target for cancer therapy: from biology to clinical use. Semin. Cancer Biol. *31*, 52–64.
15. Zatovicova, M., Jelenska, L., Hulikova, A., Ditte, P., Ditte, Z., Csaderova, L., Svastova, E., Schmalix, W., Boettger, V., Bevan, P., et al. (2014). Monoclonal antibody G250 targeting CA : binding specificity, internalization and therapeutic effects in a non-renal cancer model. Int. J. Oncol. *45*, 2455–2467.
16. Oosterwijk, E., Debruyne, F.M., and Schalken, J.A. (1995). The use of monoclonal antibody G250 in the therapy of renal-cell carcinoma. Semin. Oncol. *22*, 34–41.
17. Kappler, M., Taubert, H., Holzhausen, H.J., Reddemann, R., Rot, S., Becker, A., Kuhnt, T., Dellas, K., Dunst, J., Vordermark, D., et al. (2008). Immunohistochemical detection of HIF-1alpha and CAIX in advanced head-and-neck cancer. Prognostic role and correlation with tumor markers and tumor oxygenation parameters. Strahlenther. Onkol. *184*, 393–399.
18. Eckert, A.W., Lautner, M.H., Schutze, A., Bolte, K., Bache, M., Kappler, M., Schubert, J., Taubert, H., and Bilkenroth, U. (2010). Co-expression of Hif1alpha and CAIX is associated with poor prognosis in oral squamous cell carcinoma patients. J. Oral Pathol. Med. *39*, 313–317.
19. Capkova, L., Koubkova, L., and Kodet, R. (2014). Expression of carbonic anhydrase IX (CAIX) in malignant mesothelioma. An immunohistochemical and immunocytochemical study. Neoplasma. *61*, 161–169.
20. Chen, Z., Ai, L., Mboge, M.Y., Tu, C., McKenna, R., Brown, K.D., Heldermon, C.D., and Frost, S.C. (2018). Differential expression and function of CAIX and CAXII in breast cancer: a comparison between tumorgraft models and cells. PLoS one *13*, e0199476.
21. Pastorekova, S., Parkkila, S., Parkkila, A.K., Opavsky, R., Zelnik, V., Saarnio, J., and Pastorek, J. (1997). Carbonic anhydrase IX, MN/CA IX: analysis of stomach complementary DNA sequence and expression in human and rat alimentary tracts. Gastroenterology *112*, 398–408.
22. Saarnio, J., Parkkila, S., Parkkila, A.K., Waheed, A., Casey, M.C., Zhou, X.Y., Pastoreková, S., Pastorek, J., Karttunen, T., Haukipuro, K., et al. (1998). Immunohistochemistry of carbonic anhydrase isozyme IX (MN/CA IX) in human gut reveals polarized expression in the epithelial cells with the highest proliferative capacity. J. Histochem. Cytochem. *46*, 497–504.
23. Monti, S.M., Supuran, C.T., and De Simone, G. (2012). Carbonic anhydrase IX as a target for designing novel anticancer drugs. Curr. Med. Chem. *19*, 821–830.
24. Stillebroer, A.B., Mulders, P.F., Boerman, O.C., Oyen, W.J., and Oosterwijk, E. (2010). Carbonic anhydrase IX in renal cell carcinoma: implications for prognosis, diagnosis, and therapy. Eur. Urol. *58*, 75–83.
25. Sun, Z., Liu, B., Ruan, X., and Liu, Q. (2014). An enhanced immune response against G250, induced by a heterologous DNA primeprotein boost vaccination, using polyethyleneimine as a DNA vaccine adjuvant. Mol. Med. Rep. *10*, 2657–2662.
26. Zhao, Y., Wei, Z., Yang, H., Li, X., Wang, Q., Wang, L., and Li, S. (2017). Enhance the antirenca carcinoma effect of a DNA vaccine targeting G250 gene by co-expression with cytotoxic T-lymphocyte associated antigen-4(CTLA-4). Biomed. Pharmacother *90*, 147–152.
27. Chai, D., Zhang, Z., Jiang, N., Ding, J., Qiu, D., Shi, S.Y., Wang, G., Fang, L., Li, H., Tian, H., et al. (2021). Co-immunization with L-Myc enhances CD8(+) or CD103(+) DCs mediated tumor-specific multi-functional CD8(+) T cell responses. Cancer Sci *112*, 3469–3483.
28. Yamamoto, T., Gotoh, M., Sasaki, H., Terada, M., Kitajima, M., and Hirohashi, S. (1993). Molecular cloning and initial characterization of a novel fibrinogen-related gene, HFREP-1. Biochem. Biophys. Res. Commun. *193*, 681–687.
29. Yu, J., Li, J., Shen, J., Du, F., Wu, X., Li, M., Chen, Y., Cho, C.H., Li, X., Xiao, Z., et al. (2021). The role of Fibrinogen-like proteins in Cancer. Int. J. Biol. Sci. *17*, 1079–1087.
30. Son, Y., Shin, N.R., Kim, S.H., Park, S.C., and Lee, H.J. (2021). Fibrinogen-like protein 1 modulates sorafenib resistance in human hepatocellular carcinoma cells. Int. J. Mol. Sci. *22*, 5330.
31. Zhang, Y., Qiao, H.X., Zhou, Y.T., Hong, L., and Chen, J.H. (2018). Fibrinogenlikeprotein 1 promotes the invasion and metastasis of gastric cancer and is associated with poor prognosis. Mol. Med. Rep. *18*, 1465–1472.
32. Wang, J., Sanmamed, M.F., Datar, I., Su, T.T., Ji, L., Sun, J., Chen, L., Chen, Y., Zhu, G., Yin, W., et al. (2019). Fibrinogen-like protein 1 is a major immune inhibitory ligand of LAG-3. Cell *176*, 334–347.
33. Liu, K., and Nussenzweig, M.C. (2010). Origin and development of dendritic cells. Immunological Rev. *234*, 45–54.
34. Reis e Sousa, C. (2006). Dendritic cells in a mature age. Nat. Rev. Immunol. *6*, 476–483.
35. Yang, B., Jeang, J., Yang, A., Wu, T.C., and Hung, C.F. (2014). DNA vaccine for cancer immunotherapy. Hum. Vaccin. Immunother. *10*, 3153–3164.
36. Lopes, A., Vandermeulen, G., and Preat, V. (2019). Cancer DNA vaccines: current preclinical and clinical developments and future perspectives. J. Exp. Clin. Cancer Res. *38*, 146.
37. Chai, D., Shan, H., Wang, G., Zhang, Q., Li, H., Fang, L., Song, J., Liu, N., Zhang, Q., Yao, H., et al. (2019). Combining DNA vaccine and AIM2 in H1 nanoparticles exert anti-renal carcinoma effects via enhancing tumor-specific multi-functional CD8(+) T-cell responses. Mol. Cancer Ther. *18*, 323–334.
38. Zhang, M., Hong, Y., Chen, W., and Wang, C. (2017). Polymers for DNA vaccine delivery. ACS Biomater. Sci. Eng. *3*, 108–125.
39. Danhier, F., Ansorena, E., Silva, J.M., Coco, R., Le Breton, A., and Preat, V. (2012). PLGA-based nanoparticles: an overview of biomedical applications. J. Contr. Release. *161*, 505–522.
40. Patnaik, S., and Gupta, K.C. (2013). Novel polyethylenimine-derived nanoparticles for in vivo gene delivery. Expet Opin. Drug Deliv. *10*, 215–228.
41. Wang, X., Niu, D., Hu, C., and Li, P. (2015). Polyethyleneimine-based nanocarriers for gene delivery. Curr. Pharm. Des. *21*, 6140–6156.
42. Shau, M.D., Shih, M.F., Lin, C.C., Chuang, I.C., Hung, W.C., Hennink, W.E., and Cherng, J.Y. (2012). A one-step process in preparation of cationic nanoparticles with poly(lactide-co-glycolide)-containing polyethylenimine gives efficient gene delivery. Eur. J. Pharm. Sci. *46*, 522–529.
43. Guo, S., Xiao, P., Li, B., Wang, W., Wang, S., Lv, T., Xu, X., Chen, C., Huang, L., Li, Z., et al. (2020). Co-immunizing with PD-L1 induces CD8(+) DCs-mediated anti-tumor immunity in multiple myeloma. Int. Immunopharm. *84*, 106516.
44. Desch, A.N., Gibbings, S.L., Clambey, E.T., Janssen, W.J., Slansky, J.E., Kedl, R.M., Henson, P.M., and Jakubzick, C. (2014). Dendritic cell subsets require cis-activation for cytotoxic CD8 T-cell induction. Nat. Commun. *5*, 4674.
45. Ma, Y., Adjemian, S., Mattarollo, S.R., Yamazaki, T., Aymeric, L., Yang, H., Catani, J.P.P., Hannani, D., Duret, H., Steegh, K., et al. (2013). Anticancer chemotherapy-induced intratumoral recruitment and differentiation of antigen-presenting cells. Immunity *38*, 729–741.
46. Parajuli, N., Muller-Holzner, E., Bock, G., Werner, E.R., Villunger, A., and Doppler, W. (2010). Infiltrating CD11b+CD11c+ cells have the potential to mediate inducible nitric oxide synthase-dependent cell death in mammary carcinomas of HER-2/neu transgenic mice. Int. J. Cancer. *126*, 896–908.
47. Raskov, H., Orhan, A., Christensen, J.P., and Gogenur, I. (2021). Cytotoxic CD8(+) T cells in cancer and cancer immunotherapy. Br. J. Cancer. *124*, 359–367.
48. Park, J.S., Yang, H.N., Woo, D.G., Jeon, S.Y., Do, H.J., Lim, H.Y., Kim, J.H., and Park, K.H. (2011). Chondrogenesis of human mesenchymal stem cells mediated by the combination of SOX trio SOX5, 6, and 9 genes complexed with PEI-modified PLGA nanoparticles. Biomaterials *32*, 3679–3688.